

Original article

Effect of body mass index on shifts in ultrasound-based image-guided intensity-modulated radiation therapy for abdominal malignancies

Mehee Choi^{a,c}, Clifton D. Fuller^{a,b,c}, Samuel J. Wang^c, Ather Siddiqi^d, Adrian Wong^e, Charles R. Thomas Jr.^c, Martin Fuss^{c,a,*}

^aDepartment of Radiation Oncology, ^bDivision of Radiological Sciences, University of Texas Health Science Center at San Antonio, San Antonio, TX, USA, ^cDepartment of Radiation Medicine, Oregon Health & Science University, Portland, OR, USA, ^dUS Oncology, San Antonio, TX, USA, ^eDepartment of Diagnostic and Interventional Imaging, University of Texas Health Science Center at Houston, Houston, TX, USA

Abstract

Background and purpose: We investigated whether corrective shifts determined by daily ultrasound-based image-guidance correlate with body mass index (BMI) of patients treated with image-guided intensity-modulated radiation therapy (IG-IMRT) for abdominal malignancies. The utility of daily image-guidance, particularly for patients with BMI > 25.0, is examined.

Materials and methods: Total 3162 ultrasound-directed shifts were performed in 86 patients. Direction and magnitude of shifts were correlated with pretreatment BMI. Bivariate statistical analysis and analysis of set-up correction data were performed using systematic and random error calculations.

Results: Total 2040 daily alignments were performed. Average 3D vector of set-up correction for all patients was 12.1 mm/fraction. Directional and absolute shifts and 3D vector length were significantly different between BMI cohorts. 3D displacement averaged 4.9 mm/fraction and 6.8mm/fraction for BMI ≤ 25.0 and BMI > 25.0, respectively. Systematic error in all axes and 3D vector was significantly greater for BMI > 25.0. Differences in random error were not statistically significant.

Conclusions: Set-up corrections derived from daily ultrasound-based IG-IMRT of abdominal tumors correlated with BMI. Daily image-guidance may improve precision of IMRT delivery with benefits assessed for the entire population, particularly patients with increased habitus. Requisite PTV margins suggested in the absence of daily image-guidance are significantly greater in patients with BMI > 25.0.

© 2008 Elsevier Ireland Ltd. All rights reserved. Radiotherapy and Oncology xx (2008) xxx–xxx.

Keywords: Image-guided radiotherapy (IGRT); Patient positioning; Body mass index (BMI); Ultrasound; Intensity-modulated radiation therapy (IMRT)

Obesity is a growing problem in the industrialized world [1–4]. It is associated with increased risk for several cancer types, including cancers of the colon, endometrium, esophagus, and possibly other sites [5,6]. Several studies postulate that obesity affects biochemical pathways that in turn modulate carcinogenesis [7–9]. Given the rising prevalence of obesity, the increasing incidence of abdominal malignancies, and the etiological link between obesity and cancer, it can be readily surmised that a significant fraction of patients with abdominal malignancies will exhibit excessive body mass index (BMI), defined as weight in kg/height in meters squared, greater than 25.0.

Radiotherapy is utilized routinely for many distinct abdominal cancers, and the development of more sophisticated approaches continues to improve patient manage-

ment and outcomes [10–12]. A newly emerging treatment option is intensity-modulated radiation therapy (IMRT). The premise of IMRT depends on the ability to deliver a curative dose to the entire volume of target tumor cells while minimizing toxicity to surrounding tissue. In treating overweight/obese patients with IMRT, radiation oncologists must overcome some unique challenges presented by large body habitus. Several studies address the difficulties associated with delivery of radiation in obese patients by investigating methods to reduce the size of the planning target volume (PTV), thus maximizing efficacy and safety of radiation delivered. Image-guided IMRT (IG-IMRT) represents an attempt to reduce both systematic and random errors, and conceivably the marginal expansion of the PTV attributable to positional uncertainty, via implementation of spe-

cific strategies to more accurately assess tumor spatial location.

One IG-IMRT strategy that has seen wide implementation in prostatic cancer is ultrasound (US)-based image-guidance. Recently, data have been presented showing the utility of US IG-IMRT in hypothesis generating series for pancreatic and biliary tract lesions [13,14]. While US is a well-established modality for imaging of gastrointestinal anatomy, specific physical parameters (*i.e.* sonic transmissibility through media, greater surface/target distance) are altered by increased subcutaneous fat notable in obese patients. In the context of IG-IMRT, initial external setup accuracy may be compromised owing to increased difficulty in immobilization and external marker alignment in patients of excessive weight.

Consequently, in an effort to determine the impact of body habitus on US-derived IG-IMRT directional shifts in abdominal cancer patients, we retrospectively compared directional shift parameters in a consecutive series of patients.

Materials and methods

Chart review, data collection, and data analysis for this study were approved by the Institutional Review Board of the University of Texas Health Science Center at San Antonio (UTHSCSA).

Patient and tumor characteristics

Between September 2000 and August 2004, 86 patients completed a course of image-guided serial tomotherapeutic IMRT with daily trans-abdominal stereotactic US-based image-guidance for the treatment of abdominal malignancies. Patients were treated at the UTHSCSA Department of Radiation Oncology and the Cancer Therapy and Research Center, San Antonio, TX. Tumor location was classified as hepatic, hepatobiliary, or pancreatic. Tumor distribution by site and by histology is summarized in Table 1.

Patient selection

Included in this study were consecutive patients referred for radiation therapy for tumors in the abdomen. Prior to treatment planning computed tomography (CT) simulation, an US study was performed in the treatment position on the CT simulator table to determine whether the tumor or tumor-bearing region could be visualized. During this imaging study, guidance structures, mainly large vessels or operative clips, within the future radiation target volume or in close relation to involved organs were identified.

Patients with incomplete wound healing secondary to surgical resection or exploratory laparotomy were excluded. Although US visualization would most likely have been possible in these patients, the potential risk of wound infection due to daily abdominal manipulation and wound contamination with US gel mandated this restriction. Because diagnostic US has minimal known method-related specific health risks and can be safely applied on a daily basis, no other exclusion criteria were defined.

Table 1
Summary of tumor distribution by site/histology

Characteristic	n	%
Site		
Gallbladder/bile ducts/ampullary	21	24
Liver (metastatic)	18	21
Liver (primary)	17	20
Pancreas	28	33
Pancreas (metastatic)	2	2
All	86	100
Histology (primary site)		
Adenocarcinoma (unknown primary)	6	7
Adenocarcinoma (pancreas)	25	29
Adenocarcinoma (gallbladder/bile ducts/ampullary)	3	4
Adenocarcinoma (breast primary)	3	3
Adenocarcinoma (colon primary)	5	6
Squamous cell (gastric primary)	1	1
Adenocarcinoma (gastric primary)	2	2
Adenocarcinoma (rectal primary)	1	1
Cholangiocarcinoma/adenocarcinoma (biliary ducts)	16	19
Gangliocytic paraganglioma	1	1
Hepatocellular carcinoma	17	20
Mucinous cystadenocarcinoma	2	2
Neuroendocrine carcinoma	1	1
NHL (metastatic)	1	1
NSCLC (metastatic)	1	1
Rhabdomyosarcoma	1	1
Total	86	100

IMRT treatment planning and delivery

Imaging for treatment planning was performed on a clinical radiation therapy CT simulator with spiral option (Philips Marconi Picker PQ 5000). Image data were acquired in a slow helical scanning technique with relaxed free breathing by the patient. Images were reconstructed in contiguous 3 mm slices. To obtain optimal vascular contrast, a timed contrast bolus of 100–120 mL nonionic contrast media at a flow of 2–2.5 mL/s was applied and excellent arterial and portal venous contrast was achieved. In select cases, a second delayed helical scan was obtained to visualize the later venous contrast phase.

Following image data transfer into the treatment planning software (CORVUS[®], Nomos, Cranberry Township, PA), the gross tumor volume (GTV) and the clinical target volume (CTV) were delineated in contiguous CT slices. Organs-at-risk (OAR), such as the spinal cord, kidneys, small bowel, stomach, and normal liver, were delineated. In addition, guidance structures in close anatomic relation to the target volume were also identified and delineated with the feasibility of ultrasound visualization as a primary consideration.

Target localization using the BAT system

Details regarding daily stereotactic US alignment using the BAT US-based image-guidance system (North American Scientific/Nomos, Cranberry Township, PA) system have been reported [15]. No technical modifications to the system were required for visualization and alignment of the abdominal target volumes.

Before BAT US localization, the patient was positioned on the treatment table in the supine position using room-laser alignment to skin fiducial marks. US images were acquired in both axial and sagittal planes. CT-delineated target and guidance structure contours were then superimposed onto the actual real-time US imaged anatomy, and possible structural misalignments were assessed. The system allows for a virtual shift of the on-screen CT-derived structure outlines until a best match to the actual US anatomy is achieved. The system then indicated the table shifts required in all three principal axes to align the patient in the correct position relative to the isocenter for delivery of the respective radiation fraction. Following execution of the suggested shifts, a confirmatory US-image set was acquired to assure anatomical alignment. Couch moves were made as needed to align targets appropriately within the treatment field under the guidance of the attending physician.

Statistical analysis

Patients were grouped into two groups based on BMI, those with BMI ≤ 25.0 (underweight/normal weight patients) and those with BMI > 25.0 (overweight/obese patients).

Shift data were digitally extracted from archival patient data, matched to BMI, and recorded as composite shifts per alignment, the sum of which represented the daily shift. Directional x-, y-, and z-axis shifts were utilized to calculate a 3D magnitude vector. Directional shifts were stratified by BMI cohort (≤ 25.0 , > 25.0) and compared using parametric statistical analyses. Each room axis and 3D vector was correlated with BMI as a continuous variable using least squares regression. Likelihood of shift magnitude > 5 mm, > 10 mm, and > 20 mm was calculated and compared between BMI cohorts using Chi-square analysis. Systematic (Σ) and random (σ) error components for absolute displacement in each axis/vector were calculated, with systematic error representing the standard deviation of all patients' individual mean displacements and random error calculated as the root mean square of all patients' individual standard deviation of displacement from isocenter [16]. Systematic error was compared between BMI cohorts using Bartlett's *F*-test for homogeneity of variance. Random error was compared using a corrected *t*-test with *a priori* unequal variance assumption between cohorts.

In order to establish PTV margin suggestions for treatment in the absence of image-guidance, we implemented established recipes for target coverage [16,17]. As a measure of clinically usable margins, margins suggested by Stroom et al. were calculated as follows: $M_{ST} = 2\Sigma + 0.7\sigma$, with M_{ST} being the margin (mm) that ensures that, on average, more than 99% of the CTV should get at least 95% of the prescribed dose, being the spread of the systematic errors SD, and σ the RMS of the random errors [17]. Alternately, the recipe proposed by van Herk et al. was utilized to provide a margin ensuring minimum cumulative CTV dose of at least 95% of the prescribed dose for 90% of the patient population as: $M_{VH} = 2.5\Sigma + 0.7\sigma$, with M_{VH} being the margin (mm) that ensures these dose coverage parameters [16].

Results

In 86 patients, a total of 3162 raw shifts were performed, resulting in 2040 daily alignments (median 27 daily alignments per patient; mean alignments; range 11–42 alignments). Fig. 1 displays summary statistics for each axis/vector as an absolute value (e.g. distance from isocenter) or as a \pm value representing directional shifts. The absolute magnitude of corrective shift was most pronounced in the y-direction with a mean \pm SD of 6.9 ± 6.2 mm (Table 2). The average 3D vector of set-up correction was 12.1 ± 8.7 mm/fraction (95% CI 11.9–12.5, median 10.1 mm, range 0–43.1 mm), with 82.7%, 52.5%, and 14.3% of alignments corrected for a magnitude vector of > 5 mm, > 10 mm, and > 20 mm, respectively (Tables 2 and 3).

Thirty-seven patients had BMI ≤ 25.0 and 49 patients had BMI ≥ 25.0 . When patients were grouped according to BMI, directional and absolute shifts along all room axes and 3D vector length were statistically different, excepting absolute shifts in the x-axis. Directional shifts are provided alongside absolute magnitude of corrective shifts in Table 2 and Fig. 1 for comparison.

Systematic and random error components of the absolute shift magnitudes are presented in Table 4. For all axes and 3D vector length, systematic and random errors were reduced for underweight/normal patients compared to overweight/obese patients. Bartlett's *F*-test for homogeneity of variance showed statistically significant differences in the systematic error components in the x-, y-, z-, and 3D vectors between BMI ≤ 25 and BMI > 25 groups ($p < 0.01$). Differences in random error estimates were not significantly different in all axes/directions.

In order to establish PTV margin suggestions for treatment in the absence of image-guidance among different BMI groups, we used the margin recipe proposed by van Herk et al., which provides a minimum cumulative CTV dose of at least 95% of the prescribed dose for 90% of the patient population [16]. Using the uncertainty data collected from our patients, van Herk margins and Stroom margin recipes were calculated as described above. For all axes and 3D vector length, PTV margins were greater in BMI > 25 group compared to BMI ≤ 25 group using both margin recipes. Results are summarized in Table 5.

Discussion

Precise delivery of IMRT is hampered by multiple sources of uncertainty, or error, defined as any deviation between planned and executed treatment [18]. Sources of RT error are classically grouped as either systematic or random. One commonly used approach to account for both systematic and random errors is the expansion of the CTV with a 3D safety margin derived from daily imaging using accepted margin recipes [10,16,19]. The newly expanded volume, or PTV, is the volume that radiation doses are prescribed to ensure that the CTV is exposed daily to the prescribed dose despite the occurrence of target set-up errors.

In overweight patients, daily set-up error can be exaggerated due to greater skin motility and more variable external/internal anatomy, i.e. skin tattoos are less reliable

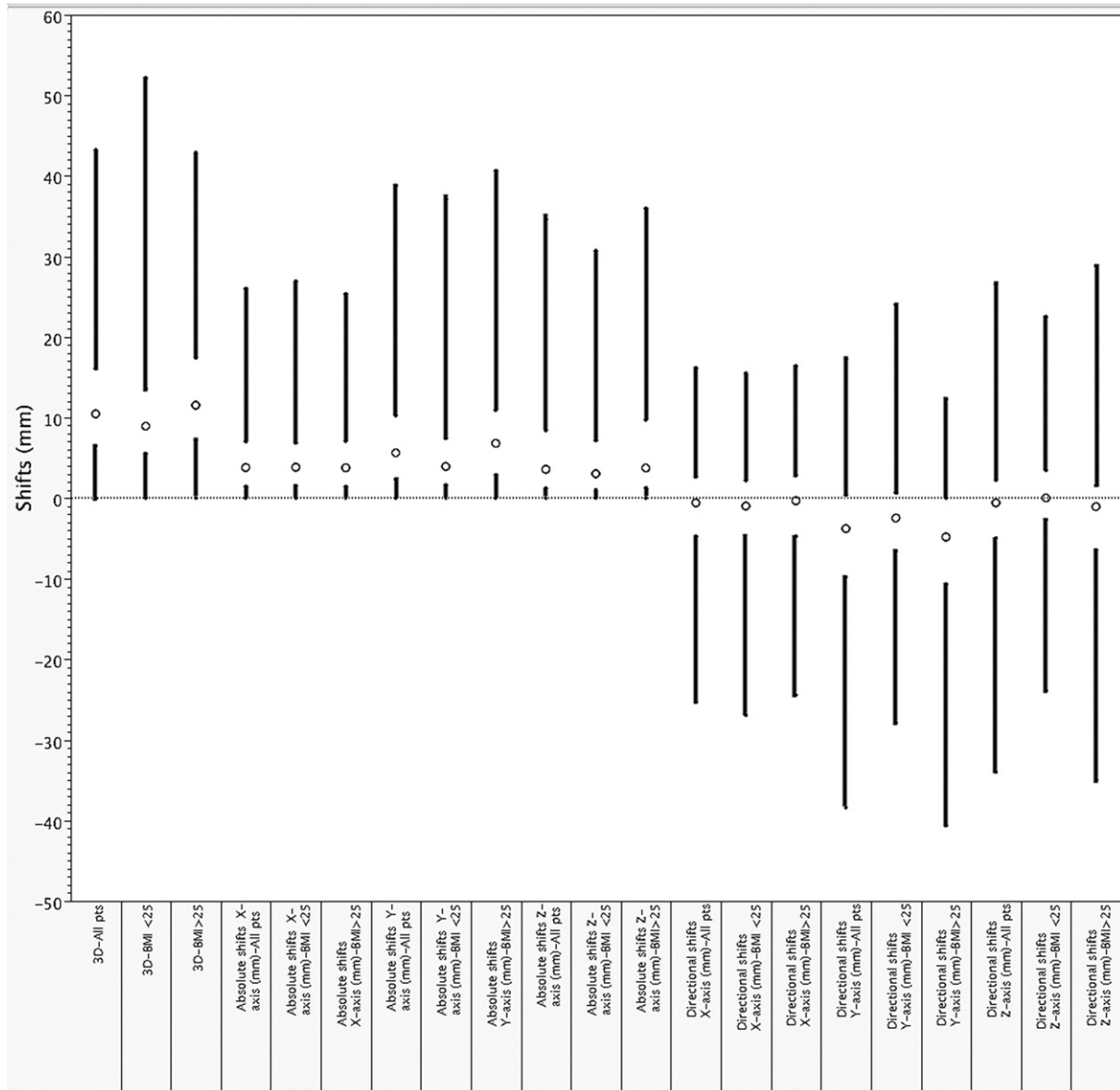


Fig. 1. Ultrasound corrective shift distributions by vector/axis by for all patients and by BMI class; mean values are represented by circles, standard deviations by gap between bars, and ranges by black bars.

due to increased mobility relative to bony structures. In a study analyzing patient and target volume set-up reproducibility in the BodyFIX double-vacuum whole body immobilization system, a significant correlation between BMI and loss of target volume coverage for obese patients (BMI > 30, $p < 0.0001$) has been reported [20]. The probability of loss of target volume dose coverage for stereotactic body radiation therapy (SBRT) treatments with narrow PTV margins was 5% at BMI 25.6, 25% at BMI 30, and 50% at BMI 32.8. In another study evaluating the setup accuracy of patients with liver metastases treated with stereotactic single dose radiation, Herfarth et al. were able to achieve high setup accuracy by using a control CT scan directly before therapy and reducing intra-corporal movement of the liver by epigastric compression [21]. The study revealed a statistically significant correlation between the mobility of the

diaphragm and BMI in male patients but not in female patients, suggesting that male-pattern distribution of intra-abdominal fat storage might account for larger shifts among heavier patients. Also critical can be the distance from the abdominal surface to the isocenter and increased thickness of tissue anterior to the target region [22,23]. With increased intra-abdominal fat, a lack of good visibility of the target region with limited ultrasound penetration might result in poorer image quality. Furthermore, there are practical limitations of radiation therapy equipment such as table weight limits and CT scan aperture limits. These technical difficulties might account, at least in part, for differences in precision of treatment delivery between BMI groups. When using conformal dose distributions, narrow margins, and steep dose gradients during IMRT, these errors can have significant detrimental effects if not corrected.

Table 2
Summary of shifts by BMI cohort

	All	BMI \leq 25	BMI > 25	<i>p</i>
Absolute shift [mean \pm SD (mm)]				
x-axis	4.9 \pm 4.6	4.7 \pm 4.5	4.9 \pm 4.7	0.29
y-axis	6.9 \pm 6.2	5.6 \pm 5.9	7.6 \pm 6.2	<0.001*
z-axis	6.2 \pm 7.4	4.9 \pm 5.6	5.6 \pm 6.2	<0.001*
3D	12.1 \pm 8.7	4.9 \pm 5.9	6.8 \pm 7.9	<0.001*
Directional shift [mean \pm SD (mm)]				
x-axis	-1.8 \pm 6.6	-1.9 \pm 6.3	-1.0 \pm 6.7	<0.001*
y-axis	-4.5 \pm 8.1	-3.3 \pm 7.5	-5.2 \pm 8.3	<0.001*
z-axis	-1.9 \pm 9.5	0.3 \pm 7.7	-3.0 \pm 10.0	<0.001*
3D	12.2 \pm 8.7	10.4 \pm 7.8	13.1 \pm 8.9	<0.001*

Abbreviations: 3D = 3-dimensional; SD = standard deviation.

Table 3
Probability of 3D shifts greater than 5, 10, and 20 mm by BMI cohort

	All	BMI \leq 25	BMI > 25	<i>p</i>
% greater than 5 mm	82.7	78.5	84.7	0.02*
% greater than 10 mm	52.5	41.1	58.2	0.02*
% greater than 20 mm	14.3	9.1	16.9	<0.01*

Abbreviations: 3D = 3-dimensional.

Table 4
Systematic and random error by BMI cohort

	All	BMI \leq 25	BMI > 25	<i>p</i>
Σ_x (mm)	3.2	2.5	3.6	<0.001 ^{a,*}
Σ_y (mm)	4.1	3.4	4.4	<0.01 ^{a,*}
Σ_z (mm)	4.0	2.5	5.6	<0.001 ^{a,*}
Σ_{3D} (mm)	5.9	4.2	6.8	<0.001 ^{a,*}
σ_x (mm)	4.5	3.9	4.6	0.48 ^b
σ_y (mm)	4.6	4.6	4.7	0.92 ^b
σ_z (mm)	5.5	5.0	5.9	0.84 ^b
σ_{3D} (mm)	6.8	6.2	6.7	0.51 ^b

Abbreviations: Σ = systematic error; σ = random error; x = x-axis; y = y-axis; z = z-axis; 3D = 3-dimensional.

^a Bartlett's *F*-test *p*-value.

^b Non-equivalent variance *t*-test *p*-value.

The data regarding body habitus and setup error are limited. Luchka addressed the challenge of set-up verification and correction based on bony anatomy by using online portal imaging devices which substantially reduced set-up error in the case of a 150 kg patient [24]. Millender and colleagues utilized daily portal imaging in combination with gold seed fiducial markers to simultaneously correct for set-up error and organ motion error in a series of three morbidly obese patients with prostate cancer. Corrective shifts of 11.4 mm/fraction, 7.2 mm/fraction, and 2.6 mm/fraction in the x-, y-, and z-directions, respectively, were observed [25].

Table 5
PTV margins by BMI cohort

	All	BMI \leq 25	BMI > 25
M_{ST}^a (mm)			
x-axis	9.5	7.8	10.7
y-axis	11.3	10.0	12.1
z-axis	12.8	7.5	15.3
3D	16.6	12.7	18.7
M_{VH}^b (mm)			
x-axis	11.1	9.0	12.5
y-axis	13.4	11.7	14.3
z-axis	15.0	8.5	18.0
3D	19.6	14.8	22.2

Abbreviations: PTV = planning target volume.

^a Stroom margin (M_{ST}) calculated via the method of Stroom and Heijmen, where $M_{ST} = 2\Sigma + 0.7\sigma$ (Σ denotes systematic error, and σ random error) [17].

^b van Herk margin (M_{VH}) calculated via the method of van Herk et al., where $M_{VH} = 2.5\Sigma + 0.7\sigma$ (Σ denotes systematic error, and σ random error) [16].

When using US-based IG-IMRT in patients of large body habitus, alterations in several specific physical parameters (*i.e.* sonic transmissibility through media, greater surface/target distance, degree of inter-user variability, movement of target by ultrasound transducer pressure) might uniquely impact error in the context of ultrasound [22,26–28].

In a recent study, our group has reported clinical feasibility of daily ultrasound-based IG-IMRT for the treatment of pancreatic cancers. Preliminary outcomes in the study supported the conclusion that this form of image-guidance may yield significant benefits with respect to target positioning, specifically, by achieving reduction in the positional variability of the target volume and allowing for a meaningful reduction of PTV safety margins [15]. Applying this method of IMRT delivery here in the treatment of obese patients for various abdominal malignancies, we were able to demonstrate average corrective shifts comparable to those previously achieved [24].

Another objective of this study was to define field margins for the construction of a PTV from a CTV for two separate patient groups, those with BMI \leq 25.0 and those with BMI > 25.0. Set-up error and organ motion error were incorporated using the margin recipe of van Herk et al. [18]. Practically speaking, 3D omni-directional, rather than asymmetric, margins are utilized for PTV expansion. PTV expansion would necessarily be significantly greater in overweight/obese patients, as compared to normal/underweight patients. In our patient population, clinically relevant translational errors were predominantly observed in obese patients with BMI > 25.0. Consequently, in the absence of daily image-guidance, the use of larger margins for patients with BMI > 25.0 may be advisable. Our findings suggest that, since setup corrections derived from daily image-guidance correlate with body habitus, daily image-guidance significantly can improve the precision of IMRT delivery, particularly in the subset of patients with BMI > 25.0; nonetheless, margin reduction through PTV decrement using IGRT should be undertaken with great care.

To our knowledge, this series represents the largest study to date of the effect of BMI on abdominal image-guidance-based positional shift differentials. However, while all tumors were located abdominally, this series included an array of tumor diagnoses. This inherent series heterogeneity might conceivably alter the applicability of resultant conclusions across all abdominal radiation target sites. As a single institution retrospective review, the standard caveats regarding archival data must be summarily noted. Additionally, the dataset herein was collected using a single imaging modality (ultrasound).

There have been differing reports on the accuracy of US-based image-guidance systems such as BAT as compared with other soft-tissue verification systems with either CT or gold seeds in prostate cancer patients [23,29–38]. Recent studies utilizing formal method comparison statistical approaches have demonstrated lack of interchangeability of ultrasound and kilovoltage X-ray-derived shifts in prostate cancer patients [30]. Researchers from Fox Chase Cancer Center recently reported prospective data showing systematic differences between BAT ultrasound and computed tomography-derived prostate shifts of <1 mm and random differences of approximately 2 mm, with average absolute differences (systemic and random) of less than 2 mm omni-directionally [29]. The degree of statistical agreement between other imaging modalities and abdominal US-guided approaches has yet to be established. In the interim, until data demonstrating statistical comparability between other imaging forms and trans-abdominal ultrasound, any speculative comparison between imaging modalities would be specious.

Proper patient positioning is critical for gaining maximum benefit and minimizing unwanted side effects of IMRT. These observations and margin recommendations have direct utility in patients with abdominal malignancies and could potentially be broadly applied to cancers localized to other regions of the body. Therefore, additional studies are warranted for specific recommendations to be made. Thus, the present data represent a useful estimation of the potential effect of body size upon the need for and the utility of daily image-guidance, and thus serves as a hypothesis generating reference for future endeavors.

Acknowledgements

C.D.F. was funded in part by UTHSCSA Graduate Division of Radiological Sciences/National Institute of Biomedical Imaging and BioEngineering Multidisciplinary Training Grant in Human Imaging (5T32EB000817-04). The funder(s) played no role in design, collection, analysis and interpretation of data, in the writing of the manuscript, nor in the decision to submit the manuscript for publication.

Portions of this dataset were presented at the ASTRO Translational Research Symposium held on September 7–8, 2007 in San Francisco, CA.

* **Corresponding author.** Martin Fuss, Department of Radiation Medicine, Oregon Health & Science University, 3181 SW Sam Jackson Park Road, KPV4, Portland, OR 97239-3098, USA. *E-mail address:* fussm@ohsu.edu

Received 16 November 2007; received in revised form 30 July 2008; accepted 9 August 2008

References

- [1] WHO. Obesity: preventing and managing the global epidemic. Report of a WHO consultation. World Health Organ Tech Rep Ser 2000;894:i–xii, 1–253.
- [2] Ogden CL, Carroll MD, Curtin LR, et al. Prevalence of overweight and obesity in the United States, 1999–2004. *Jama* 2006;295:1549–55.
- [3] Silventoinen K, Sans S, Tolonen H, et al. Trends in obesity and energy supply in the WHO MONICA Project. *Int J Obes Relat Metab Disord* 2004;28:710–8.
- [4] Flegal KM, Carroll MD, Ogden CL, et al. Prevalence and trends in obesity among US adults, 1999–2000. *Jama* 2002;288:1723–7.
- [5] Bianchini F, Kaaks R, Vainio H. Overweight, obesity, and cancer risk. *Lancet Oncol* 2002;3:565–74.
- [6] James PT. Obesity: the worldwide epidemic. *Clin Dermatol* 2004;22:276–80.
- [7] Kaaks R, Lukanova A. Energy balance and cancer: the role of insulin and insulin-like growth factor-I. *Proc Nutr Soc* 2001;60:91–106.
- [8] Hursting SD, Lavigne JA, Berrigan D, et al. Calorie restriction, aging, and cancer prevention: mechanisms of action and applicability to humans. *Annu Rev Med* 2003;54:131–52.
- [9] Ngo TH, Barnard RJ, Leung PS, et al. Insulin-like growth factor I (IGF-I) and IGF binding protein-1 modulate prostate cancer cell growth and apoptosis: possible mediators for the effects of diet and exercise on cancer cell survival. *Endocrinology* 2003;144:2319–24.
- [10] Verellen D, De Ridder M, Storme G. A (short) history of image-guided radiotherapy. *Radiother Oncol* 2008;86:4–13.
- [11] Sultana A, Tudur Smith C, Cunningham D, et al. Systematic review, including meta-analyses, on the management of locally advanced pancreatic cancer using radiation/combined modality therapy. *Br J Cancer* 2007;96:1183–90.
- [12] Czito BG, Hurwitz HI, Clough RW, et al. Adjuvant external-beam radiotherapy with concurrent chemotherapy after resection of primary gallbladder carcinoma: a 23-year experience. *Int J Radiat Oncol Biol Phys* 2005;62:1030–4.
- [13] Fuss M, Wong A, Fuller CD, et al. Image-guided intensity-modulated radiotherapy for pancreatic carcinoma. *Gastrointest Cancer Res* 2007;1:2–11.
- [14] Fuller CD, Thomas Jr CR, Wong A, et al. Image-guided intensity-modulated radiation therapy for gallbladder carcinoma. *Radiother Oncol* 2006;81:65–72.
- [15] Fuss M, Salter BJ, Cavanaugh SX, et al. Daily ultrasound-based image-guided targeting for radiotherapy of upper abdominal malignancies. *Int J Radiat Oncol Biol Phys* 2004;59:1245–56.
- [16] van Herk M, Remeijer P, Rasch C, et al. The probability of correct target dosage: dose-population histograms for deriving treatment margins in radiotherapy. *Int J Radiat Oncol Biol Phys* 2000;47:1121–35.
- [17] Stroom JC, Heijmen BJ. Geometrical uncertainties, radiotherapy planning margins, and the ICRU-62 report. *Radiother Oncol* 2002;64:75–83.
- [18] van Herk M. Errors and margins in radiotherapy. *Semin Radiat Oncol* 2004;14:52–64.
- [19] Parker W, Esmerelda Poli M, Patrocinio H, et al. An assessment of inter-fraction prostate motion based on 10,327 pre-treatment ultrasound localizations for 387 prostate cancer patients treated with conformal 3D external beam radiation therapy (EBRT). *Radiother Oncol* 2006;80:59.
- [20] Fuss M, Salter BJ, Rassiah P, et al. Repositioning accuracy of a commercially available double-vacuum whole body immobilization system for stereotactic body radiation therapy. *Technol Cancer Res Treat* 2004;3:59–67.

- [21] Herfarth KK, Debus J, Lohr F, et al. Extracranial stereotactic radiation therapy: set-up accuracy of patients treated for liver metastases. *Int J Radiat Oncol Biol Phys* 2000;46:329–35.
- [22] Serago CF, Chungbin SJ, Buskirk SJ, et al. Initial experience with ultrasound localization for positioning prostate cancer patients for external beam radiotherapy. *Int J Radiat Oncol Biol Phys* 2002;53:1130–8.
- [23] McNair HA, Mangar SA, Coffey J, et al. A comparison of CT- and ultrasound-based imaging to localize the prostate for external beam radiotherapy. *Int J Radiat Oncol Biol Phys* 2006;65:678–87.
- [24] Luchka K, Shalev S. Pelvic irradiation of the obese patient: a treatment strategy involving megavoltage simulation and intra-treatment setup corrections. *Med Phys* 1996;23:1897–902.
- [25] Millender LE, Aubin M, Pouliot J, et al. Daily electronic portal imaging for morbidly obese men undergoing radiotherapy for localized prostate cancer. *Int J Radiat Oncol Biol Phys* 2004;59:6–10.
- [26] McGahan JP, Ryu J, Fogata M. Ultrasound probe pressure as a source of error in prostate localization for external beam radiotherapy. *Int J Radiat Oncol Biol Phys* 2004;60:788–93.
- [27] Langen KM, Pouliot J, Anezinos C, et al. Evaluation of ultrasound-based prostate localization for image-guided radiotherapy. *Int J Radiat Oncol Biol Phys* 2003;57:635–44.
- [28] Dobler B, Mai S, Ross C, et al. Investigation of possible prostate displacement due to ultrasound positioning in external radiation therapy. *Radiother Oncol* 2005;76:S217.
- [29] Feigenberg SJ, Paskalev K, McNeeley S, et al. Comparing computed tomography localization with daily ultrasound during image-guided radiation therapy for the treatment of prostate cancer: a prospective evaluation. *J Appl Clin Med Phys* 2007;8:2268.
- [30] Fuller CD, Thomas CR, Schwartz S, et al. Method comparison of ultrasound and kilovoltage x-ray fiducial marker imaging for prostate radiotherapy targeting. *Phys Med Biol* 2006;51:4981–93.
- [31] Lattanzi J, McNeeley S, Donnelly S, et al. Ultrasound-based stereotactic guidance in prostate cancer – quantification of organ motion and set-up errors in external beam radiation therapy. *Comput Aided Surg* 2000;5:289–95.
- [32] Lock M, Wong E, Bauman G, et al. Evaluation of 3D-ultrasound image-guided radiotherapy in prostate cancer compared to implanted fiducial markers. *Radiother Oncol* 2005;76:S4.
- [33] Peignaux K, Truc G, Barillot I, et al. Clinical assessment of the use of the Sonarray system for daily prostate localization. *Radiother Oncol* 2006;81:176–8.
- [34] Scarbrough TJ, Golden NM, Ting JY, et al. Comparison of ultrasound and implanted seed marker prostate localization methods: implications for image-guided radiotherapy. *Int J Radiat Oncol Biol Phys* 2006;65:378–87.
- [35] Tirona R, Morton G, Pearse M, et al. Interfraction motion measured using 3D ultrasound and gold seed localization. *Radiother Oncol* 2006;80:S48.
- [36] Tomé W, Orton N, Jaradt H, et al. On the use of 3D-ultrasound localization systems for in room imaging. *Radiother Oncol* 2006;78:S13.
- [37] Van den Heuvel F, Powell T, Seppi E, et al. Independent verification of ultrasound based image-guided radiation treatment, using electronic portal imaging and implanted gold markers. *Med Phys* 2003;30:2878–87.
- [38] Vandepuut V, Hermans J, Bussels B, et al. Daily ultrasound-based prostate localization: can we reduce the margins for prostate motion? *Radiother Oncol* 2004;73:S181–2.